2018

Modeling of S-RAM Energy Recover Compressor Integration in a Transcritical Carbon Dioxide Cycle for Application in Electronics Cooling in Varying Gravity

Riley Barta
Purdue University, bartar@purdue.edu

Jason J. Hugenroth
S-RAM Dynamics, United States of America, jason@s-ram.com

Eckhard A. Groll
Purdue University - Main Campus, groll@purdue.edu

Modeling of S-RAM Energy Recover Compressor Integration in a Transcritical Carbon Dioxide Cycle for Application in Electronics Cooling in Varying Gravity

Riley B. BARTA[1*], Jason J. HUGENROTH[2], and Eckhard A. GROLL[1]

[1]Ray W. Herrick Laboratories, School of Mechanical Engineering, Purdue University
West Lafayette, Indiana, 47906, USA
bartar@purdue.edu; groll@purdue.edu

[2]S-RAM Dynamics
Franklin, Tennessee, 37064, USA
jason@s-ram.com

ABSTRACT

As electronics in military aircraft are increasing in complexity, additional cooling is necessary to enable efficient and high computing performance. In addition, the varying forces that a military aircraft endures during maneuvering and inverted flight introduce unique design constraints to the electronics cooling systems. Since the cooling system for such an application will be in an aircraft, the capacity and unique design constraints must all be met with a design that is lightweight, robust, oil-free, and resistant to varying gravity. This paper presents a study comparing the coefficient of performance (COP) of several cooling cycles utilizing both R134a and carbon dioxide (CO_2) as the working fluids. Cycles with single-stage and two-stage compression with intercooling are compared, and both are modeled with suction-to-liquid-line internal heat exchangers (IHX). The cycles utilizing CO_2 are transcritical to reach the required temperatures for heat rejection from the gas cooler. Additionally, CO_2 cycles with expansion work recovery and an ejector are compared. The cooling requirements are up to 150 kW with a heat source temperature as low as 1.7 ℃ and a cooling airflow inlet temperature of 48.9 ℃ at an air mass flow rate of 9.1 kg/s. The purpose of this analysis is to understand which of these cycles performs with the highest efficiency for the given electronics cooling application and results in a higher air outlet temperature to potentially reduce the necessary temperature lift for a cascaded air cycle.

1. INTRODUCTION

With increasing interest in natural refrigerants, the heating, ventilation, air conditioning, and refrigeration (HVAC&R) industry has placed a large importance on the development of technologies that utilize these fluids and minimize performance losses. While a disadvantage of CO_2 is the high pressures and transcritical operation necessary for adequate heat rejection to a heat sink at a temperature above the critical point, its performance can be competitive with existing hydrofluorocarbon (HFC) cycles if its cycle is properly designed using cycle enhancing measures. Some of these cycle enhancements include an internal suction-to-liquid-line heat exchanger (IHX), an expander, or an ejector. Additionally, because CO_2 has a negligible global warming potential (GWP), high volumetric heat capacity, and is non-explosive, it is beneficial for use in future military applications. The temperature glide match between the heat rejected from CO_2 in the gas cooler to a counter-flow airstream can also lead to a larger airside temperature lift, which can be helpful in cascade cycle applications.

Lorentzen (1994) first suggested the revival of CO_2, and cited the refrigerant being non-toxic, incombustible, and low cost, among several other advantages that would benefit military application. Brown *et al.* (2001) performed a theoretical analysis comparing CO_2 and R134a for automotive air conditioners and found that, while the CO_2 cycle COP was lower than the R134a cycle COP by up to 34%, the approach temperature between the air and CO_2 during heat rejection was over 50% smaller than the approach temperature in the R134a cycle. Although the smaller approach temperature in the case of CO_2 did not offer enough performance benefit to overcome the cycle performance disparity, it was concluded that a counter-flow gas cooler may offer additional performance benefits for the CO_2 cycle over a cross-flow gas cooler if glide matching with the external heat-transfer fluid was utilized.

Expansion work recovery has been a focus of researchers aiming to increase the efficiency of transcritical CO_2 cycles. For instance, Robinson and Groll (1998) analyzed two transcritical CO_2 cycles with and without expansion work

recovery by means of thermodynamic models. Results showed that the cycle employing an expansion work recovery device with an isentropic efficiency of 60% had a 25% higher COP than the cycle without an expansion work recovery device but with maximum internal heat exchange. Zhang *et al.* (2007) developed a double acting free piston expander for power recovery in a transcritical CO_2 cycle and predicted a theoretical isentropic efficiency of 62% when applied in a transcritical CO_2 cycle by means of a P-V diagram obtained during initial testing with air. Baek *et al.* (2002) designed and tested a prototype piston-cylinder expansion device in a transcritical CO_2 cycle and increased the system performance by up to 10% even though the efficiency of the expander was only approximately 17%. Yang *et al.* (2009) experimentally evaluated a rotary vane expander in a transcritical CO_2 cycle and, through analysis of internal losses, were able to improve the volumetric and isentropic efficiencies from 17% to 30% and 9% to 23%, respectively.

Another technology suitable for transcritcal CO_2 applications that has been under development by both researchers and manufacturers is an ejector, which can reduce the load on compressors by increasing the suction pressure without penalizing cycle functionality. Li and Groll (2005) developed a model for an ejector applied in a transcritical CO_2 refrigeration cycle and found that the cycle COP can be improved by more than 16% over a basic transcritical CO_2 cycle. To the best of the authors' knowledge, a patent by Gay (1931) is credited with the invention of the two-phase ejector used in a refrigeration system, and the design was further improved by Newton (1972) and Kemper *et al.* (1996). Elbel and Hrnjak (2008) experimentally tested a prototype ejector with a variable nozzle in a transcritical CO_2 cycle and achieved increases in cooling capacity and COP of up to 8% and 7%, respectively. Lee *et al.* (2011) designed a prototype ejector and analyzed the effects of varying the motive throat diameter, the distance between the motive nozzle and diffuser, as well as the mixing section diameter. These variations allowed the authors to identify physical parameters within the ejector that would lead to a favorable increase in cycle performance for a given operating condition, ultimately resulting in a COP up to 15% higher than that of a conventional transcritical CO_2 air conditioning cycle.

In this paper, a novel Energy Recovery Compressor (ERC) that utilizes the Sanderson-Rocker Arm Mechanism (S-RAM) is one of the primary technologies proposed in a transcritical CO_2 cycle for an electronics cooling application. In particular, the S-RAM converts reciprocating motion to rotary motion, without the sidewall losses often seen with crankshaft, wobble plate, or swash plate drive mechanisms. Additionally, the S-RAM drive can vary piston stroke without altering the head clearance. Given the variable gravity considerations in this application, the ERC will need to be an oil-free design. A more in-depth description of the S-RAM, as well as an analysis and experimental result of a transcritical CO_2 compressor that utilizes the S-RAM can be found in Kurtulus et al. (2014). The multi-piston device can be configured so that some pistons are used for compression, while others are used for expansion.

More specifically, an overview of the performance airflow of six vapor-compression cycles using either CO_2 or R134a with heat source temperatures as low as 1.7 ℃ and a cooling airflow inlet temperature of 48.9 ℃ at a mass flow rate of 9.1 kg/s is presented and discussed. The effects of the cycle architectures on the cooling airflow outlet temperature are considered because future applications may include employing this cycle as a low-temperature cycle that will then reject heat to a high-temperature air cycle. Therefore, a higher air outlet temperature from cooling of the vapor-compression cycle can reduce the necessary temperature lift on the air cycle. Advantages and disadvantages of the two working fluids and the several cycle designs are outlined in order to identify new research opportunities.

2. DESCRIPTION OF CYCLES EVALUATED

A total of six vapor compression cycle configurations were considered in this analysis. The schematics are illustrated in Figure 1a through Figure 1f. In particular, four cycles employed CO_2 as the working fluid and the remaining two cycles utilized R134a. All two-stage cycles featured intercooling between the first and second stages of compression. Two of the CO_2 cycles utilized both the ERC to recover expansion work and an IHX.

By analyzing the different cycles in more details, the following main characteristics can be identified:

- Figure 1a and Figure 1b illustrate single-stage and two-stage CO_2 cycles, respectively, with ERCs and IHXs.
- Figure 1c and Figure 1d represent single-stage and two-stage CO_2 cycles, respectively, with ejectors and without IHXs.
- Figure 1e and Figure 1f show single-stage and two-stage R134a cycles, respectively, with electronic expansion valves (EXVs) for isenthalpic expansion, and IHXs.

The decision of whether or not to use an IHX was made by comparing all six cycles with and without and IHX, and choosing the design that yielded the highest COP.

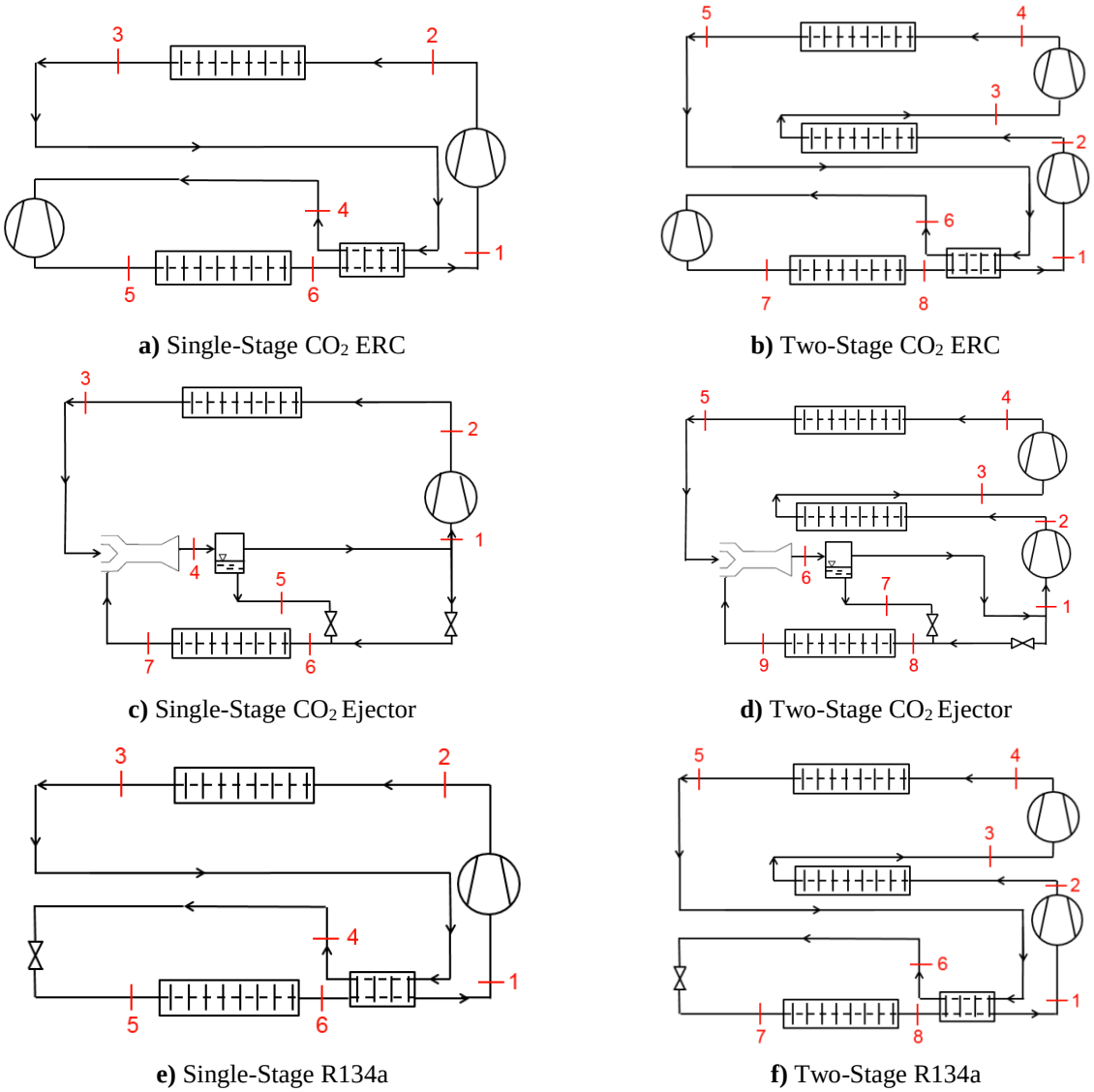

a) Single-Stage CO_2 ERC

b) Two-Stage CO_2 ERC

c) Single-Stage CO_2 Ejector

d) Two-Stage CO_2 Ejector

e) Single-Stage R134a

f) Two-Stage R134a

Figure 1: Overview of Cycle Configurations

3. METHODOLOGY

3.1 System Analysis

The primary method used to assess the performance of the various cycles analyzed is the coefficient of performance (COP). Since the purpose of this cycle is cooling, the definition of COP is the ratio of cooling capacity to net power input, as expressed by Equation 1.

$$COP = \frac{\dot{Q}_{cool}}{\dot{W}_{net}} \tag{1}$$

In the case of CO_2 cycles that utilize expansion work recovery, $\dot{W}_{Exp}$, the net power input is given by Equation 2.

$$\dot{W}_{net} = \dot{W}_{Comp} - \dot{W}_{Exp} \tag{2}$$

In the two-stage cycles, $\dot{W}_{Comp}$ is the sum of the power consumed by the two compressors. Additionally, for CO_2 cycles the gas cooler pressure is varied to maximize COP at a given operating condition, as is the intercooling pressure for both CO_2 and R134a two-stage cycles.

The system analyses were performed using Engineering Equation Software (EES) as developed by Klein (2018). The models were developed to assess steady-state performances. While COP was the primary method of quantifying performance, CO_2 and R134a were also assessed on the outlet temperature of the air used to cool the condenser or gas cooler, for R134a and CO_2, respectively. While the evaporator simply pulls heat from an assumed low-temperature sink, the high-temperature heat rejection occurs from the refrigerant to an air stream, allowing a comparison of the effects of the temperature glide of each respective refrigerant against the air on system performance.

In the proposed ERC, the expansion work recovery device utilizes the potential energy in the high-pressure CO_2 at the gas cooler outlet and recovers that potential energy through expanding the refrigerant in a cylinder and driving a piston. The energy that the piston recovers while the volume of the refrigerant increases is fed directly to the shaft that drives the cylinders performing the compression, thus reducing the net power consumption of the system. Alternatively, an ejector uses a motive nozzle to convert the high-pressure CO_2 at the gas cooler outlet into a high-velocity flow. This high-velocity flow then draws the suction flow from the evaporator outlet into a mixing chamber before exiting through a diffuser to the compressor suction. The mixing and diffusion processes increase the pressure of the refrigerant above the evaporation pressure before separating the phases of the flow and sending saturated vapor to the compressor, which reduces the amount of compressor input work needed. The ejector cycle model was developed utilizing the strategy outlined in Li and Groll (2005), which isolates the motive and suction nozzle outlet states, the mixing state, and the diffuser outlet state.

3.2 Baseline Parameters and Assumptions

The operating conditions in this analysis involve a low-temperature heat source from which the cycle absorbs heat and a high-temperature air stream that the cycle rejects heat to. Two heat source temperatures, along with the inlet air stream parameters and system cooling capacity are given in Table 1. An evaporator outlet superheat of 5 ℃ was assumed, and for the R134a cycle a condenser outlet subcool of 5 ℃ was assumed. A minimum internal pinch, or temperature difference between air and refrigerant, was assumed to be 5 ℃ for R134a and 2.5 ℃ for CO_2.

Table 1: Design Operating Conditions

$T_{low,min}$ [℃]	$T_{low,max}$ [℃]	$T_{air,in}$ [℃]	$\dot{m}_{air}$ [kg/s]	$\dot{Q}_{cool}$ [kW]
1.7	10.0	48.9	9.1	150

Equations for the compressor and expander isentropic efficiency are shown in Equations 3 and 4, respectively.

$$\eta_{is,Comp} = \frac{h_{out,is} - h_{in}}{h_{out} - h_{in}} \tag{3}$$

$$\eta_{is,Exp} = \frac{h_{in} - h_{out}}{h_{in} - h_{out,is}} \tag{4}$$

where the outlet specific enthalpy for an isentropic expansion is calculated as

$$h_{out,is} = f(p_{out}, s_{in}) \tag{5}$$

In the case of the ejector cycle, isentropic efficiencies need to be assumed for the motive nozzle, suction nozzle, and the diffuser. The nozzle efficiency calculation given in Equation 6 was applied for both the motive and suction nozzles, and the diffuser efficiency equation is given in Equation 7. Isentropic efficiencies of 70% were assumed for the expander and compressor, 80% for the ejector diffuser, and 90% for the motive and suction nozzles in the ejector.

$$\eta_{is,Nozzle} = \frac{h_{in} - h_{out}}{h_{in} - h_{out,is}} \tag{6}$$

$$\eta_{is,Diffuser} = \frac{h_{out,is} - h_{in}}{h_{out} - h_{in}} \tag{7}$$

3.3 Heat Exchanger Modeling Strategy

The evaporator was modeled simply based on a heat source model. Therefore, the refrigerant temperature through the evaporator was calculated as a function of the heat source temperature, evaporator outlet superheat, and pinch, shown in Equation 8.

$$T_{Evap} = T_{source} - T_{superheat} - T_{pinch} \tag{8}$$

Because the high-temperature side rejects heat to an air stream, a segmented counter-flow heat exchanger model was used to find the outlet states of both the air stream and the refrigerant. A diagram outlining this strategy is shown in Figure 2.

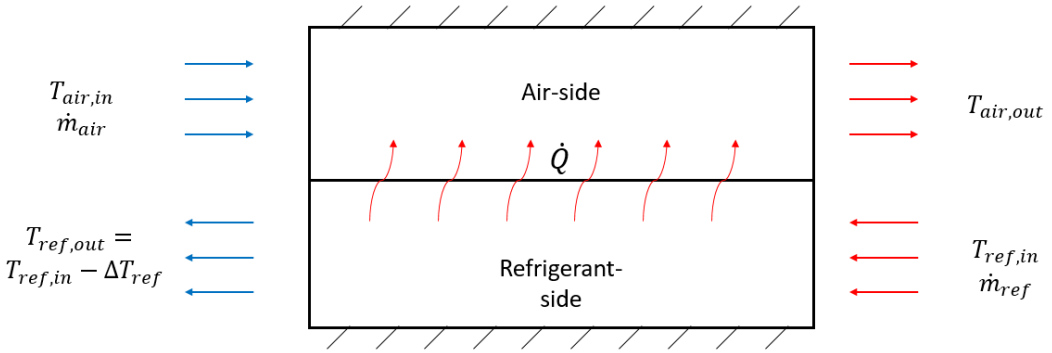

Figure 2: Segmented Counter-Flow Heat Exchanger Modeling Diagram

The model assumed that the heat exchanger was adiabatic, resulting in 100% of the heat rejected from the refrigerant being absorbed by the air stream. Given the inlet air temperature, air mass flow rate, the refrigerant inlet temperature, and the minimum internal pinch, the outlet states of the refrigerant and airflow were found through Equation 9.

$$\dot{m}_{ref}\left(h_{ref,in} - h_{ref,out}\right) = \dot{m}_{air}(h_{air,out} - h_{air,in}) \tag{9}$$

A segmented heat exchanger modeling approach is taken because it is important to consider the difference between internal pinch and the pinch at the outlet of the heat exchanger. For CO_2, the refrigerant remains in a supercritical state for the entirety of the heat rejection process due to its critical point of 31 °C and the air inlet temperature being 48.9 °C. Therefore, the minimum temperature difference between the CO_2 and airflow occurs at the gas cooler outlet, allowing the calculation of the gas cooler outlet temperature with Equation 10.

$$T_{GasCooler,out} = T_{air,in} + T_{pinch,int} \tag{10}$$

Because the R134a heat rejection occurs at a sub-critical state and thus, most of the heat rejection occurs in the two-phase region, the minimum temperature difference between R134a and the air stream does not occur at the outlet of the condenser, but rather at the point where the R134a transitions from superheated vapor to a two-phase state. Therefore, the condenser temperature is solved through Equation 11, where $T_{pinch,Cond}$ is iterated upon until a value is found that results in an internal pinch point, $T_{pinch,int}$, of 5 °C.

$$T_{Cond} = T_{air,in} + T_{subcool} + T_{pinch,Cond} \tag{11}$$

Figures 3 and 4 show the temperature change for both CO_2 and R134a, respectively, against the air stream temperature change in the counter-flow heat exchanger model employed in this analysis. The x-axis label of numerical steps represents the partitions of the heat exchanger that were analyzed individually. The air enters at numerical step 100, while the refrigerant enters at numerical step 0.

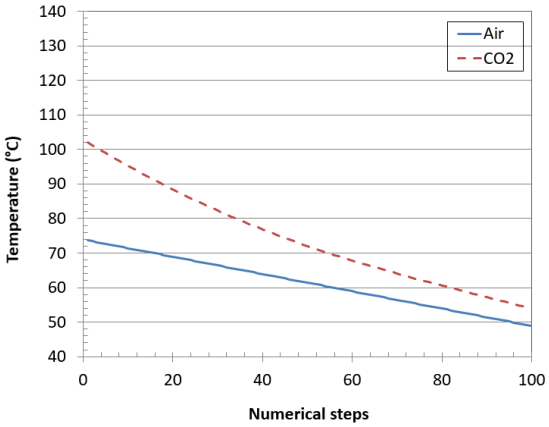

Figure 3: CO_2 and Air Counter-Flow Temperatures

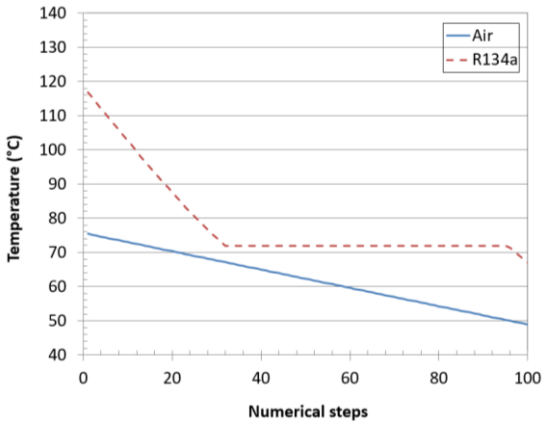

Figure 4: R134a and Air Counter-Flow Temperatures

Because of the consideration of airside properties, attention needed to be paid to the orientation of the intercooler relative to the gas cooler or condenser in the two-stage cycles. The constraint of $\dot{m}_{air} = 9.1$ kg/s allowed only three options for heat exchanger orientation. The first option was to leave the heat exchangers in parallel, and simply distribute the airflow as a function of refrigerant-side heat rejection rate. The second option was to place the intercooler upstream of the condenser such that the air outlet temperature from the intercooler is the air inlet temperature for the condenser, but both heat exchangers get the full mass flow rate of air. The third and final option was to place the condenser upstream of the intercooler such that the condenser air outlet temperature is the intercooler air inlet temperature while both heat exchangers still get the full mass flow rate of air. For the cycles that employ an IHX, an effectiveness, ε, of 90% is assumed. The heat transfer is limited by the difference between the low-pressure and high-pressure inlet temperatures so that the low-pressure outlet temperature does not exceed the high-pressure inlet temperature. Once the heat transfer rate through the IHX is calculated, the outlet state of the IHX on both the high-pressure and low-pressure sides can be found.

4. RESULTS AND DISCUSSION

4.1 Cycle Performance Results

The cycle configurations are compared in terms of thermodynamic cycle plots and COP. In particular, P-h diagrams for the single-stage and two-stage CO_2 ERC cycles are shown in Figures 5a and 5b, respectively. P-h diagrams for all cycles include operation at heat source temperatures of 1.7 ℃ and 10.0 ℃. The two-stage CO_2 ERC cycle resulted in a 11.1% and 10.7% higher COP relative to the single-stage CO_2 ERC cycle for heat source temperatures of 1.7 ℃ and 10.0 ℃, respectively. Both heat source temperatures were analyzed for single-stage and two-stage CO_2 ejector cycles as well and the corresponding P-h diagrams are shown in Figures 5c and 5d, respectively. The two-stage CO_2 ejector cycle resulted in a 4.9% and 3.0% higher COP for heat source temperatures of 1.7 ℃ and 10.0 ℃, respectively than the single-stage CO_2 ejector cycle. The R134a cycles were analyzed in the same way, and P-h diagrams of both single and two-stage R134a cycles are shown in Figures 5e and 5f, respectively. The two-stage R134a cycle resulted in a 3.3% and 2.8% higher COP than the single-stage R134a cycle for heat source temperatures of 1.7 ℃ and 10.0 ℃, respectively. If only comparing cycles with the same number of compression stages, the CO_2 cycles have a lower COP than the R134a cycles for the same operating conditions. The closest performance occurs between the two-stage CO_2 ERC cycle and the two-stage R134a cycle at a source temperature of 10.0 ℃, where the CO_2 cycle COP is 5.5% lower than the R134a cycle. The COP results for all cycles analyzed are reported in Table 2.

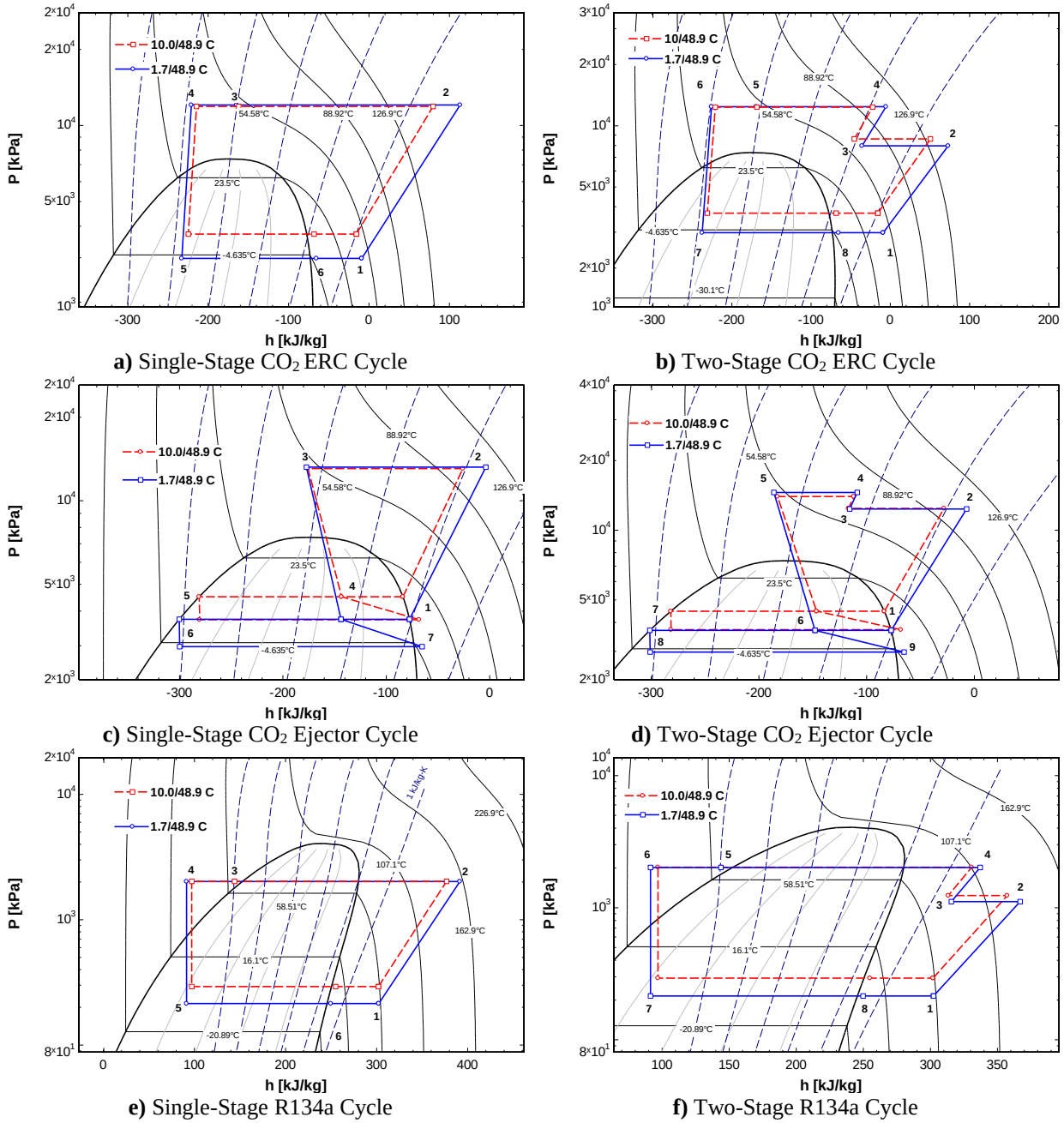

a) Single-Stage CO_2 ERC Cycle

b) Two-Stage CO_2 ERC Cycle

c) Single-Stage CO_2 Ejector Cycle

d) Two-Stage CO_2 Ejector Cycle

e) Single-Stage R134a Cycle

f) Two-Stage R134a Cycle

Figure 5: Overview of Cycle P-h Diagrams

Table 2: Cycle COP Results

Cycle	$T_{low} = 1.7$ [℃]	$T_{low} = 10.0$ [℃]
Single-Stage CO_2 ERC	1.52	1.83
Two-Stage CO_2 ERC	1.71	2.05
Single-Stage CO_2 Ejector	1.35	1.59
Two-Stage CO_2 Ejector	1.42	1.64
Single-Stage R134a	1.78	2.11
Two-Stage R134a	1.84	2.17

4.2 Airside Results

The single-stage heat exchanger airside modeling was straightforward because there was only one heat exchanger, being either the condenser in the case of R134a or the gas cooler for CO_2 cycles. Therefore, that heat exchanger received both the heat sink air inlet temperature as well as the full mass flow rate of air. For the two-stage cycles, modeling showed that placing the condenser upstream of the intercooler in series resulted in the highest COP for the two-stage cycles analyzed. Thus, this orientation was chosen to be implemented for all three two-stage cycles. In addition to the heat exchanger orientation analysis, the air outlet temperature for all cycles analyzed in this paper was calculated to offer insight on how various vapor-compression cycle architectures and working fluids could affect the airside results. If the cycle were to be used as a low-temperature cycle cascaded with a high-temperature cycle with air as the working fluid, understanding the air outlet temperature would have a direct impact on the temperature lift across the air cycle. Therefore, the air outlet temperatures for all six cycles analyzed are tabulated in Table 3.

Table 3: Cycle Air Outlet Temperature Results

Cycle	Air Outlet Temperature	
	$T_{low} = 1.7$ [℃]	$T_{low} = 10.0$ [℃]
Single-Stage CO_2 ERC	76.1	74.2
Two-Stage CO_2 ERC	74.8	73.3
Single-Stage CO_2 Ejector	77.3	75.5
Two-Stage CO_2 Ejector	76.8	75.2
Single-Stage R134a	74.5	73.0
Two-Stage R134a	74.2	72.8

5. CONCLUSIONS

The purpose of this analysis was to determine the most suitable cycle architecture that yielded the best performance and the most favorable airside outlet temperature in an electronics cooling application in military aircraft for two working fluids. Four CO_2 cycles and two R134a cycles were analyzed that featured an ejector, an ERC, an EXV, single-stage compression, and two-stage compression with intercooling. Based on the numerical analyses, it can be concluded that the CO_2 ejector cycles could not compete with the CO_2 ERC or R134a cycles. Therefore, it was not necessary to solve the issues of phase separation in varying gravity situations. While the two-stage CO_2 ERC cycle showed higher performance than the single-stage, a maximum of 11.1% COP improvement may not justify the added cost and complexity of the second compressor and intercooler. For the two-stage design at a heat source temperature of 10.0 ℃, the R134a cycle COP was only 5.5% higher than that of the two-stage CO_2 ERC cycle at the same heat source condition, representing the cycle and operating condition combination that resulted in the closest performance to the R134a cycle by a CO_2 cycle. The maximum difference in air outlet temperatures between the two working fluids was found comparing the single-stage CO_2 ejector with the single-stage R134a cycle, where the air outlet temperature for the CO_2 cycle was 3.6% higher than that of the R134a cycle. Future work will focus on increasing the complexity

of the heat exchanger model to more accurately model airside effects, and also to build in an empirical expander and compressor model for the CO_2 ERC.

ACKNOWLEDGEMENTS

The authors would like to thank S-RAM Dynamics for technical and financial support, the faculty and staff of Ray W. Herrick Laboratories for technical support for this project, and the U.S. Department of Defense for financial support through an SBIR Grant.

REFERENCES

Baek, J.S., Groll, E.A., Lawless, P.B. (2002). Development of a Piston-Cylinder Expansion Device for the Transcritical Carbon Dioxide Cycle. *Proc. Of the Int'l Compressor Eng. Conf. at Purdue,* Paper 584, West Lafayette, IN, 2002.

Brown, J.S., Yana-Motta, S.F., Domanski, P.A. (2001). Comparative Analysis of an Automotive Air Conditioning Systems Operating with CO_2 and R134a. *International Journal of Refrigeration, 25:1, 19-32.*

Elbel, S., Hrnjak, P. (2008). Experimental Validation of a Prototype Ejector Designed to Reduce Throttling Losses Encountered in Transcritical R744 System Operation. *International Journal of Refrigeration, 31:3, 411-422.*

Gay, N.J. (1931). Refrigerating System. U.S. Patent No. 1,836,318.

Kemper, G.A., Harper, G.F., Brown, G.A. (1996). Multiple Phase Ejector Refrigeration System. U.S. Patent No. 3,277,660.

Klein, S., "Engineering Equation Solver", F-Chart Software, v. 10.268, 2018.

Kurtulus, O., Yang, B., Lumpkin, D., Groll, E.A., Jestings, L., and Conde, R. (2014). Performance and Operating Characteristics of a Novel Positive-Displacement Oil-Free CO2 Compressor. *Proc. Of the Int'l Compressor Eng. Conf. at Purdue,* Paper 2375, West Lafayette, IN, July 14-17, 2014.

Lee, J. S., Kim, M. S., Kim, M. S. (2011). Experimental Study on the Improvement of CO_2 Air Conditioning System Performance Using an Ejector. *International Journal of Refrigeration, 34:7, 1614-1625.*

Li, D., Groll, E.A. (2005). Transcritical CO_2 Refrigeration Cycle with Ejector-Expansion Device. *International Journal of Refrigeration, 28:5, 766-773.*

Lorentzen, G. (1994). Revival of Carbon Dioxide as a Refrigerant. *International Journal of Refrigeration, 17:5, 292-301*.

Newton, A.B. (1972). Capacity Control for Multiple-Phase Refrigeration Systems. U.S. Patent No. 3,670,519.

Robinson, D. M., Groll, E. A. (1998). Efficiencies of Transcritical CO_2 Cycles with and without an Expansion Turbine. *International Journal of Refrigeration, 21:7, 577-589.*

Yang, B., Peng, X., He, Z., Guo, B., Xing, Z. (2009). Experimental Investigation on the Internal Working Process of a CO_2 Rotary Vane Expander. *Applied Thermal Engineering, 29:11-12, 2289-2296.*

Zhang, B., Peng, X., He, Z., Xing, Z., Shu, P. (2007). Development of Double Acting Free Piston Expander for Power Recovery in Transcritical CO_2 Cycle. *Applied Thermal Engineering, 27:8-9, 1629-1636.*

NOMENCLATURE

T	Temperature	(℃)	**Greek Symbols**	
P	Pressure	(kPa)	η	Efficiency
h	Specific Enthalpy	(kJ/kg)	ε	Effectiveness
ṁ	Mass Flow Rate	(kg/s)	**Subscript**	
s	Specific Entropy	(kJ/(kg-K))	Comp	Compressor

$\dot{W}$	Power	(kW)	Exp	Expander
$\dot{Q}$	Heat Transfer Rate	(kW)	in	Inlet
Acronyms			out	outlet
COP	Coefficient of Performance		is	Isentropic
IHX	Internal Heat Exchanger		Evap	Evaporator
ERC	Energy Recovery Compressor		Cond	Condenser
S-RAM	Sanderson Rocker Arm Mechanism		ref	Refrigerant
EES	Engineering Equation Solver		int	Internal
EXV	Electronic Expansion Valve		low	Low-Side
GWP	Global Warming Potential		subcool	Subcooling